Benefits of a Nonsynchronous Microgrid on Dense-Load LV Secondary Networks

Reynaldo Salcedo, *Student Member, IEEE*, Abdullah Bokhari, Marc Diaz-Aguiló, Nanzhu Lin, Tianqi Hong, Francisco de León, *Fellow, IEEE*, Dariusz Czarkowski, *Member, IEEE*, Shalom Flank, Alan McDonnell, and Resk Ebrahem Uosef, *Member, IEEE*

***Abstract*—This paper describes the advantages of using nonsynchronous microgrids in networked systems containing densely concentrated loads. The nonsynchronous bus arrangement, in addition to allowing for the integration of substantially larger distributed generation, completely isolates transient disturbances from and to the network and the microgrid. Significant is the fact that distributed generators installed in the microgrid do not contribute to the short-circuit current that needs to be interrupted by the substation breakers. The behavior of the grid and the microgrid is investigated by comparing: the occurrence of faults, voltage reduction, and losses, in the presence and absence of the microgrid. The benefits of the dc microgrid are made evident with steady-state and transient studies performed on a real distribution network in New York City.**

***Index Terms*—CVR, distributed generation, microgrid, nonsynchronous interconnection.**

I. Introduction

NONSYNCHRONOUS microgrids offer an effective solution for the interconnection of distributed energy resources, loads, and storage [1]. Previous research has shown the importance of microgrids [2]–[5] and the usage of ac-dc-ac links [6], [7]. A quantitative study evaluating dc microgrids statistically showed a potential for power availability of about 0.999, called 3-nines [9], [10]. A loss reduction of 10% to 22% over ac systems was shown in [11] and [12].

Recent trends introduced hybrid microgrids that comprise a dc bus and an ac microgrid interconnected by power-electronic interfaces [3], [13], [14]. While dc microgrids have an operational advantage over ac microgrids, protection systems and standards are more mature for ac systems than for dc systems [6], [15]. However, dc-bus based systems do not have synchronization, reactive power flow, power quality, frequency control, and stability issues [16].

The advantage of dc microgrids over ac microgrids has been highlighted in many studies [2], [7]–[11], [16]–[20] and can be summarized as: 1) easier to build and integrate with different power sources, including dc sources; 2) flexible scalability; 3) higher efficiency; 4) lower losses from the sources to loads due to the elimination of multiple power conversion stages and filtering requirements; 5) compatible for future energy uses, such as electric vehicles; 6) facilitating the integration of modern electronic loads, energy storage devices, and DG technologies; possibility for volume and cost reduction [2], [9], [17].

Several articles present simulations of dc microgrids in residential [6], [17], [21], [22]; commercial [23], [24]; and industrial [25] applications. The advanced control architecture for the successful implementation of microgrid requires a high-frequency pulsewidth-modulated control with fine resolution [26]. Phase-shift control [27] and fuzzy control [28] are other techniques used in microgrid applications [27]. Considered to be a small-scale version of a conventional interconnected power system, a microgrid is distinguished from the utility by its philosophy of operation, presence of distributed energy resources, and requirements for fast islanding [30].

In this paper, a nonsynchronous microgrid connected via a dc bus to a low-voltage (LV) ac distribution network is presented. Since an active rectifier is the only interface between the utility and the microgrid, including onsite generation, the utility is electrically isolated and only connected nonsynchronously to the microgrid. Therefore, the microgrid looks like a resistive load from the utility's perspective [29]. The objective of this paper is to evaluate the benefits of a nonsynchronous microgrid for heavily meshed networked utility grids.

This paper proposes a nonsynchronous microgrid to be implemented in the medium-voltage (MV) side of a networked grid in (Brooklyn) New York City. Steady-state and transient analyses are performed to show the virtues of the proposed microgrid topology. The behavior of the grid and the microgrid is investigated by comparing the occurrence of faults, conservation voltage reduction, and losses in the presence and absence of the microgrid. Simulations were performed using OpenDSS [31] for steady-state studies and the Electromagnetic Transients Program (EMTP) [32] for time-domain studies.

Manuscript received September 27, 2014; revised January 24, 2015; accepted April 02, 2015. Date of publication April 14, 2015; date of current version May 20, 2016. Paper no. TPWRD-01187-2014.

R. Salcedo was with the Department of Electrical and Computer Engineering at New York University, Brooklyn, NY 11201 USA . He is now with the Massachusetts Institute of Technology: Lincoln Laboratory, Lexington, MA 02421 USA (email: rsalcedo@mit.ll.edu).

A. Bokhari, M. Diaz-Aguiló, N. Lin, T. Hong, F. de León, and D. Czarkowski are with the Department of Electrical and Computer Engineering, New York University, Brooklyn, NY 11201 USA (e-mail: abdullah.bokhari@gmail.com; marc.diaz.aguilo@gmail.com; nanzhulin@nyu.edu; th1275@nyu.edu; fdeleon@nyu.edu; dcz@poly.edu).

S. Flank and A. McDonnell are with Pareto Energy Ltd., Washington DC 20037 USA (e-mail: SFlank@ParetoEnergy.com; AMcdonnell@paretoenergy.com).

R. E. Uosef is with Consolidated Edison Inc., New York, NY 10003 USA (e-mail: uosefr@coned.com).

Color versions of one or more of the figures in this paper are available online at http://ieeexplore.ieee.org.

Digital Object Identifier 10.1109/TPWRD.2015.2420594

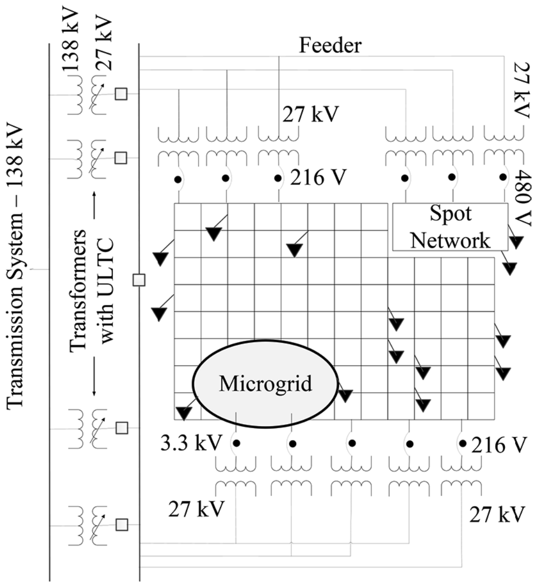

Fig. 1. Basic interconnection of the overall distribution network. The microgrid is similar to a spot network.

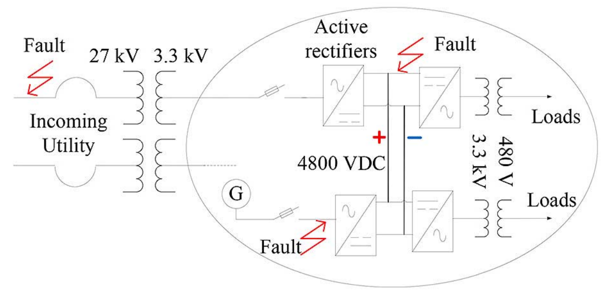

Fig. 2. Basic architecture of the nonsynchronous microgrid.

The basic interconnection of the network under investigation is shown in Fig. 1. The area substation is composed of five transformers 138/27 kV, three capacitor banks, and 52 bus breakers and feeder breakers. The voltage of the substation transformers is controlled using line drop compensation (LDC) in the under-load tap changers (ULTCs). There are thousands of primary sections that energize hundreds of network transformers connected to the secondary grid or spot networks. Nearly 10 000 secondary mains feed several thousands of distributed loads.

Due to the growing requirements of electrical power quality and reliability in urban areas such as New York City, utility companies must operate networks conservatively. In downtown areas of densely populated cities, it is typical for distribution transformers to be interconnected on the LV side by means of network protectors forming a grid, often heavily meshed, that eventually increases service continuity and reliability due to redundancy [38]. Network protectors are LV CBs whose operation prevents the continuous flow of reverse power (backfeeding from the secondary grid into the primary network) [38], [39]. The operation of these devices is instrumental for system reliability, especially in the event of a fault on an MV feeder.

II. Description of the Novel Microgrid

The architecture of the nonsynchronous microgrid under investigation was originally proposed in [44] under the name of GridLink. A simplified diagram of the microgrid design is given in Fig. 2. One of the key drivers in developing this approach has been the ability to use a "cut-and-splice" implementation. Only the transformers need to change voltage, but nothing upstream on the Con Edison 27-kV feeders needs to change when the microgrid is installed. Equally important, only the transformers on the building loads need to change, but nothing else in each building's electrical rooms needs to change either.

Preliminary financial analysis for a roughly similar 5-MW system at a site in Brooklyn indicates that investors could achieve a 25% internal rate of return on the capital required to construct a 5-MW nonsynchronous microgrid, with the end users paying about 15% to 20% less than the commercial cost of power. This arrangement provides several advantages to current distribution system infrastructures, especially to networks having fast-growing concentrated loads and substation circuit breakers (CBs) reaching short-circuit duty limitations. In a typical New York City distribution network, the short-circuit power is close to the capacity of the breakers. This often forces the utility to prevent the installation of distributed resources in its system. Otherwise, the generator owner would have to finance the cost of any system upgrades [45]. These issues may be overcome with the benefits of using nonsynchronous microgrid technologies as discussed and demonstrated in this paper by means of steady-state and transient studies.

Each nonsynchronous microgrid of the type shown in the diagram is connected toward the end of three heavily loaded utility medium-voltage (MV) feeders (of about 40-MW total-load service capacity). The step-down transformers connecting the utility system with the microgrid are rated 5 MVA 27/3.3 kV at 60 Hz. The three independent microgrid units are coordinated via high-speed communication providing N-2 redundancy as required by Con Edison for distribution systems. The active rectifiers at the input to the dc buses have sufficient filtering capabilities to mitigate switching voltage spikes and comply with voltage distortion standards [43]. Three synchronous generators rated 5 MW operating at 50 Hz are connected to each individual dc bus via active rectifiers. Because of the microgrid topology, several inverters can be connected at the dc buses providing customers with multiple line feeds for reliability and continuity of services. The voltage can be stepped-down from 3.3 kV to the utilization level by network transformers configured with primary windings connected in delta and secondary windings in grounded-wye. Although Fig. 2 shows the microgrid loads connected as spot networks; it is possible to create a low-voltage (LV) secondary grid for distributed loads as presented in [40].

A. Benefits of Flexible and Rapid Current Control

The key factors of the nonsynchronous microgrid scheme offering effective advantages to distribution system over ac microgrids are the dc power conversion, the fast power electronic switches, and the broad spectrum of possible control algorithms available when all ac systems (utility, cogeneration and load) operate independently of each other. Basic operation of power-electronic converters permits the control of current in relatively small windows of time; usually a fraction of a millisecond. The flexibility of controlling current along with the topology of operation proposed in [44] provides substantial benefits, such as ensuring unidirectional power flow into the load side by controlling the ON/OFF pulsing patterns of the switches. Unidirectional power flow is required for interconnecting with a distribution system while preventing the occurrence of continuous current reversal into the MV feeder (backfeeding condition); therefore, eliminating power oscillations, voltage-quality issues, as well as possible impacts to the upstream utility system. Moreover, current flow can be forced to be in phase with voltage such that the microgrid ideally appears as a resistive load at the utility terminals. Finally, since the microgrid is designed to operate in zero-export mode, the active rectifiers are not required to be IEEE Standard 1547 certified, increasing the range of vendors [42].

B. Benefits of Nonsynchronous Interconnection

Another important aspect of microgrids is the nonsynchronous interconnection over traditional synchronized ac systems. Therefore, disturbances or power-quality (PQ) issues within a local system do not propagate and affect other systems. All types of distributed resources may be interconnected without system impacts. Also, equipment operating at different frequencies can safely interact without jeopardizing reliability or stability. In addition, because of the asynchronous interconnection and the unidirectional power flow (import only) features of the topology, islanding is guaranteed to never be an issue—the microgrid is essentially always islanded. Approvals for installation (or expansion) of cogeneration can therefore be expedited. Ensuring nonexport conditions and negligible fault contribution further reduces the risk of rejection or delay, even when distribution feeders have reached maximum power penetration of distribution generation [45]. Although essentially islanded, the microgrid is capable of operating connected or islanded from the main grid as defined by the DOE and CIGRÉ [50], [51]. When grid connected, the zero-export condition prevents current backfeed to the utility system complying with design requirements. For islanded situations, the microgrid supplies the load using available generation while voltage and frequency within the system are locally controlled.

An economic analysis by some authors of this paper concludes that the capital cost for a roughly similar 10-MW nonsynchronous microgrid is approximately U.S.$5 million lower than the cost for a comparable traditional synchronous-connected distributed generation system [52]. This lower upfront cost does not include additional benefits, such as shortening the utility approval process, providing UPS-quality power, or reusing the same equipment to also provide equivalent export capacity.

C. Benefits During the Short Circuit on an MV Feeder

Backfeeding during a fault on an MV feeder may impose catastrophic conditions to the system infrastructure, such as prolonged faults and long duration overvoltages [41]. For these reasons, it is important for utilities to assess any possible backfeeding conditions in their system.

In the event of a short circuit, the nonsynchronous microgrid immediately eliminates the occurrence of backfeeding by implementing a fault detection system that operates and isolates the faulted MV feeder in a fraction of a cycle. The fault detection operates based on undervoltage conditions with measurements on the upstream MV feeders. Using the advantage provided by power-electronic converters for fast switching of current, it is possible to achieve complete fault isolation in a relatively small timeframe. Although this method of fault detection would prevent reverse currents well before current magnitudes reach the pickup level of the overcurrent relays, proper settings must be applied to the voltage monitoring system to avoid unintended (nuisance) tripping.

III. Steady-State Behavior

This section is devoted to analyzing the steady-state performance of a microgrid installation in a densely loaded LV secondary network. Microgrids are beneficial to reduce voltage violations on geographical zones with LV pockets and to help relieve overloaded feeders [31]. However, other benefits often dismissed are the increase in flexibility to allocate power generation and the energy savings by reducing losses in the system [31]. Without a microgrid, it is simple to allocate power generation by installing DGs scattered around the network. Although this configuration seems more flexible, it poses problems with short-circuit currents and overvoltage situations. Since these two configurations are the most plausible to allocate extra power in a given network, this paper explores their performance. All simulation results are compared with the network base case which does not have a microgrid or DG installations.

A. Description of Study Scenarios

Three different scenarios are analyzed as follows.

1) Base-Case Scenario: This scenario represents the network densely loaded and before the addition of a microgrid or scattered DG. Results from this case serve as a reference framework for the simulation of upgrades in the system.

2) Microgrid Scenario: This scenario represents the network upgraded with a microgrid. As previously described, the microgrid is composed of three individual generators of 5 MW each. Therefore, simulation cases of the microgrid will assume a total generation of 5, 10, or 15 MW. In normal operation, the utility serves the microgrid as a lumped load that is equal to the demand of all loads connected to the microgrid plus the internal losses of the microgrid (wiring and subsystems) minus the internal generation.

3) DG Scenario: This scenario models the performance of the network when DGs are not concentrated in the microgrid but are scattered across the geographical area occupied by the microgrid. This serves to address the case where individual customers, and possibly the utility, have distributed generation installed at particular locations. The objective is to represent scenarios that are comparable in power penetration to the microgrid scenarios. Therefore, cases with a total generation ranging from 1 to 15 MW are analyzed. Since the number of possible scenarios is very large for each generation level, an equivalent DG case is computed by randomizing the position and size of 20 DG units and then averaging the results of these cases. All DG units will have a unity power factor and we have maintained the number of units fixed to 20 because the variation of this number does not affect the results. For each generation level, 20 different

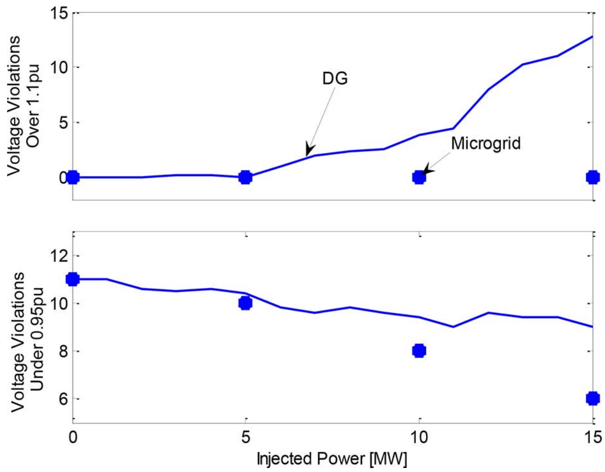

Fig. 3. Voltage violations with no voltage reduction applied as a function of injected power for the DG scenarios (solid line) and the microgrid scenario (dot). The top plot represents the 1.1-p.u. overvoltage violations and the bottom plot represents the 0.95-p.u. undervoltage violations.

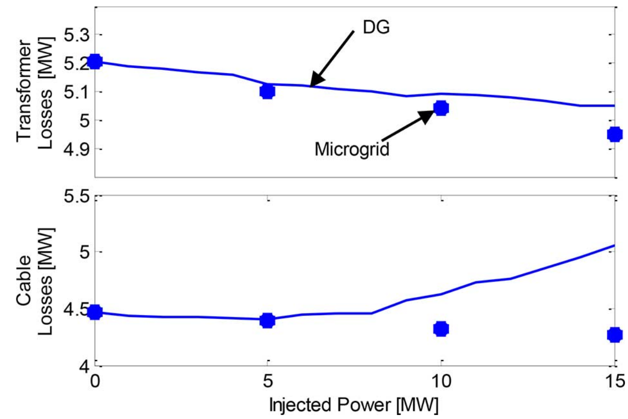

Fig. 4. Total losses in cables and transformers with no voltage reduction applied for the DG scenarios (solid line) and the microgrid scenarios (dot).

DG scenarios are computed. This has been found to be the minimum number of random scenarios to ensure a convergent average response of the network in terms of voltage violations; see [35]. The randomization is performed as follows: 1) the location of the 20 DG units is randomly set within the area of study and this randomization is applied by using a normal statistical distribution amongst the connection points in such an area and 2) the power supplied by each DG unit is also distributed with a normal statistical distribution.

B. Voltage Violation Analysis

Voltage violations are defined as voltages with a deviation exceeding $\pm 5\%$ from rated voltage during normal operating conditions and $\pm 10\%$ for emergency conditions [42]. A discussion covering voltage violations results is presented for each described scenario.

1) Overvoltage Violations: In the base-case scenario, no overvoltage violations are present in the system. In the DG cases, the number of overvoltage violations increases with the total power injected because the DG units boost the voltage locally [32], [33]. On the other hand, in the microgrid case, there are no overvoltage violations reported, demonstrating the valuable advantage of a microgrid implementation over scattered DGs due to the efficient regulation of voltage by the dc system despite the decrease of the network's power factor [32]. These behaviors can be observed from the top plot of Fig. 3.

2) Undervoltage Violations: In the DG scenarios, the undervoltage violations (voltages under 0.95 p.u.) decrease when the total injected power increases [33]. Similarly, the microgrid helps reduce undervoltage violations as the injected power increases. The microgrid scenario is more effective at reducing undervoltage violations than the DG implementation. This is due to the electrical isolation created by the dc bus. Thus, the microgrid is capable of boosting the voltage at all points within this area to the desired voltage level. Voltage violations occur for peak load conditions in LV pockets that are located far from the microgrid area. Also, it is important to note that the DG scenarios and microgrid scenarios do not present voltage violations under 0.90 p.u.

C. Loss Analysis

The major sources of loss in a system are transformer and cable losses. For the example under study, cable losses are around 1.5% of the total demand of the system and the losses in transformers represent around 2%. Both of these losses are analyzed for the DG and microgrid scenarios.

1) Losses in Cables: In the DG scenarios, as long as the injected power increases, the overall network demand decreases and, as a consequence, there will be a reduction in cable losses [34], [36]. This behavior is observed in the top plot of Fig. 4 from 0 to 5 MW. However, in certain cases with the LDC mechanism, the reduction in demand results in a reduction of the tap at the substation transformers. Therefore, the voltage on the secondary side is reduced and the series losses increase. This is observed for the DG cases in the same figure from 5 up to 15 MW power injections. For the microgrid, the total losses in cables decrease because the overall demand of the system decreases (as was previously mentioned, the internal losses of the microgrid system are not included in Fig. 4).

2) Losses in Transformers: The microgrid and DG cases demonstrated significant transformer loss reduction in comparison to the base case. This reduction of losses is a result of the decrease in system loading, which reduces the transformer tap. Both scenarios present a transformer loss reduction of approximately 4%. Internal efficiencies of the microgrid subsystems are not computed in steady state because the microgrid is modeled as a single lumped load.

D. Voltage Reduction Analysis

In this section, the performance of the microgrid is compared to the scattered DG scenarios in voltage reduction situations. Previous literature describes conservation voltage reduction (CVR) as an effective means to reduce energy in dense-load low-voltage secondary networks, but undervoltage violations may occur [34], [37].

1) Voltage Violation Analysis: This part analyzes the performance of the system when voltage reduction operations with

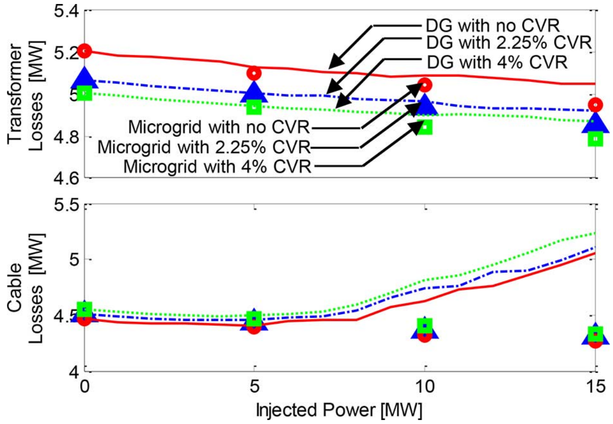

Fig. 5. Loss analysis with voltage reduction conducted for DG scenarios and microgrid scenarios.

a voltage reduction of 2.25% and 4% are conducted (these are the typical voltage reduction percentages used by the utility). To evaluate the performance of the system, the undervoltage violations below 0.9 p.u. are observed. In the scenario where 2.25% of voltage reduction is applied, the system does not present any undervoltage violations in the microgrid or the DG scenarios. For 4% of voltage reduction, the system behaves similar for microgrid and DG, reducing the number of voltage violations from eight nodes (base case) to seven nodes (microgrid and DG scenarios). This is because the DG and the microgrid only help to reduce violations in their "electrically-nearby" region and, in this particular case, only one violation occurred in the surrounding area of the microgrid.

2) Cable Losses Analysis: When voltage reduction is applied, the voltage profile in the network is reduced. As a consequence, the current circulating through the majority of the grid increases and, therefore, the series losses increase (see Fig. 5) [34]. As previously mentioned, large power allocation caused the LDC settings of the transformers to reduce the tap position and, consequently, the series losses would increase as a function of DG penetration. The top plot of Fig. 5 shows the effect of voltage reduction for three different voltage reduction levels of 0%, 2.25%, and 4%.

3) Transformer Losses Analysis: The transformer losses (including losses of substation and distribution transformers) for different cases are compared in Fig. 5. The losses are presented as a function of allocated power penetration for different voltage reduction levels. For a larger percentage of voltage reduction, a substantial decrease in transformer losses is observed. For the case of 4% voltage reduction, there is a relative difference in transformer losses of 4% in comparison to the case where voltage reduction is not applied [34]. The advantages of voltage reduction may be combined with the reduction of transformer losses caused when DG penetration increases. In the case of a presence of a microgrid of 15 MW, the transformer losses can be further reduced an extra 4%. The combination of microgrid and voltage reduction would result in a total reduction of transformer losses of 8%. This behavior can be observed in the bottom plot of Fig. 5.

E. Steady Benefits and Conclusions

By comparing the performance of microgrids and DG units in a densely loaded secondary network, it was possible to observe two advantages of microgrid systems over individual DG penetration. First, microgrids are a more advantageous and flexible alternative to allocate onsite generation and control voltage violations in the network. Also, microgrids can help reduce undervoltage violations while allowing network operation at a lower voltage, thus reducing the transformer losses in the system. Also, microgrids relieve loading on feeders by generating and delivering energy within the isolated nonsynchronous system, therefore reducing the series losses in the system. Furthermore, microgrid systems, when combined with voltage reduction operations, proved to be beneficial to enhance the overall efficiency of the network. The results show that for a 15-MW microgrid operating together with 2.25% voltage reduction would reduce transformer losses by 4.5% and series losses by 2%. The microgrid would be able to operate year round because, as opposed to configurations with individual DG units, overvoltage violations in low-load conditions are avoided by the microgrid. These enhanced voltage reduction operations, in a network with a total yearly consumption of approximately 550 GWh, would lead to yearly savings of around U.S.$200 000 and to gains in system efficiency. The total losses reduce from 3.5% to 3.38% (a 3.5% reduction) [46].

IV. Transient Behavior

Several time-domain simulations have been performed to analyze the dynamic behavior of the nonsynchronous microgrid when installed in a secondary distribution network. These simulations consider three cases:

- Case 1) three-phase short circuit at a utility MV feeder;
- Case 2) three-phase short circuit at the terminals of a microgrid onsite generator;
- Case 3) short circuit at the microgrid dc bus.

Each case intends to address utility safety and operational concerns regarding the integration of a nonsynchronous microgrid into the network. Some of these concerns include: potential short-circuit contribution from the microgrid into the upstream network, the effect of fluctuations on the generators, possible voltage instability at the utility and the customer connection points, power-quality issues at customer terminals in case of contingencies, and compliance with the interconnection conditions of IEEE Standard 519.

These transient studies show the benefits of installing nonsynchronous microgrids in meshed distribution networks during faults. For example, the case of a short circuit at the MV feeder demonstrates the microgrid capability to rapidly isolate faults, preventing significant current backfeed into the primary system which is highly beneficial to utilities. In addition, the proposed configuration permits the allocation of substantial DG, reduces load interruptions during faults, and provides improvements of voltage quality. Conversely, traditional network topology allows for current reversal lasting approximately 6 cycles until the network protectors disconnect. Furthermore, the traditional configuration places restrictions on the amount of DG penetration in the system due to fault contributions that may exceed the short-circuit rating of substation CBs.

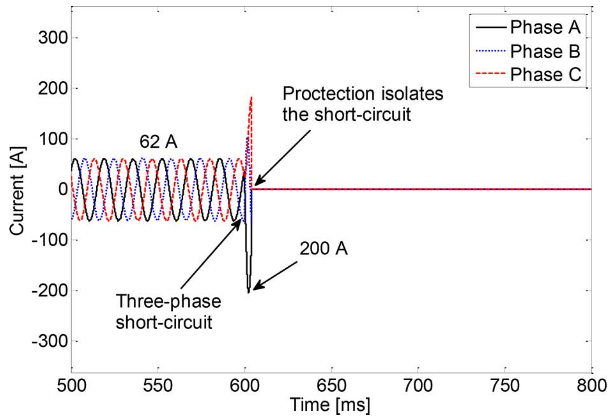

Fig. 6. Instantaneous current at the MV side of the faulted transformer.

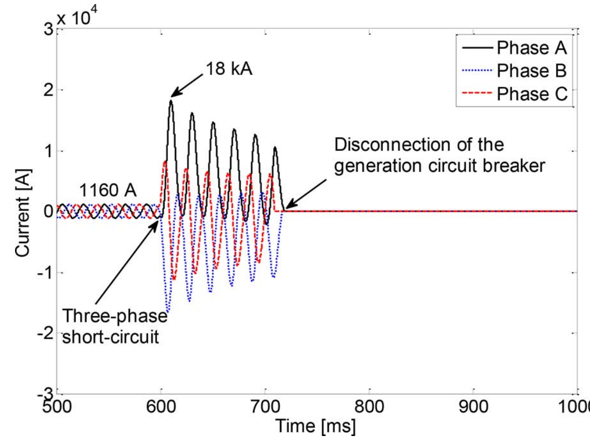

Fig. 7. Instantaneous current output of a generator during a three-phase fault at its terminal.

To start, the network is assumed to operate in steady-state conditions with nodal voltages within 5% of nominal voltage. Before applying the fault, the voltage and current waveforms were observed to be sinusoidal (without harmonic distortion). Measurements at the generators and load terminals were sinusoidal and complied with the requirements of power-quality standards [43]. The three-phase short circuits occur at approximately 600 ms of simulation time, after the system fully stabilizes.

A. Short-Circuit Studies at the Utility Side

The major concern with a short circuit on the utility side relates to possible current backfeeding from the microgrid into the MV feeders. To show the impact of a nonsynchronous microgrid during an upstream short circuit, the primary of a main power transformer connecting the utility system into the microgrid was selected as the fault location (see Fig. 2). A fault on the MV side of a main power transformer is the worst case scenario for possible backfeeding current from the microgrid. The instantaneous current waveform as observed through the primary winding of the faulted transformer is shown in Fig. 6. When the fault occurs (at 600 ms), the fault detection system immediately senses an undervoltage condition and switches off the corresponding converter within one half of a cycle, significantly eliminating backfeeding current. Most off-the-shelf controlled rectifiers can accomplish this disconnection in a smaller time frame; say one-fourth of a cycle or less [47]. The MV feeder briefly experiences, at most, the first peak of reverse current (nearly 200 A) from the microgrid. Once the fault is isolated, the remaining feeders and generators will pick up the load originally supplied by the disconnected line.

As shown, the nonsynchronous microgrid does not affect the short-circuit capabilities of the upstream network. Moreover, it may provide a delay to the upgrades of substation CBs which would have normally been required using typical paralleling of DGs with the utility system. In a conventional distribution network without a nonsynchronous microgrid, a short circuit on an MV feeder serving the area would produce a considerable voltage dip at the load terminals, probably restarting computers and other sensible equipment. In contrast to the classic distribution infrastructure, the nonsynchronous microgrid would prevent this decrease in voltage as a result of the separation of ac systems. Therefore, voltage and current at the load terminals remain constant and sinusoidal throughout the simulation, further demonstrating power-quality improvements and the "always-islanded" nature of a nonsynchronous microgrid.

B. Short Circuit at a DG Terminal

The simulation of a three-phase fault on the terminal of a generator serving the microgrid provides an insight of the advantages obtained with the nonsynchronous interconnection between ac systems. The instantaneous output current of the faulted generator observed at its terminals is shown in Fig. 7. It has a prefault value of 1160 A. The shape of this current depicts the classic decaying response of a synchronous machine to a three-phase short circuit. The microgrid system is protected by a circuit breaker that opens at approximately 650 ms of the simulation followed by the generator protection which opens at approximately 700 ms. Although the fault could have been rapidly isolated from the microgrid using similar fault detection as implemented for the MV feeder network, it is desirable to use typical protection equipment and its inherited delays to analyze the behavior of the dc microgrid when briefly sustaining a fault, and its impact to the load and the upstream system.

The contribution of the microgrid to the fault current is presented in Fig. 8. As can be noted from the plot, before the fault occurs, the current flowing into the microgrid was 1160 A. At the moment of the fault, the current reverses and flows from the microgrid to the fault with an asymmetrical shape and a first peak of approximately 2600 A. During the first half, a cycle after the short circuit appears in the network, and the dc bus voltage of the associated rectifier drops from 4800 to 4300 V. Then, it recovers with a combination of a linear response when the microgrid feeds the fault and oscillations when the short circuit is isolated from the microgrid; see Fig. 9. When the oscillations are most significant, the current of the corresponding MV feeder (see Fig. 10) shows minor disturbances as a result of the load change and the instability of the dc bus voltage. The current in the MV feeder is illustrated in Fig. 10. The current swing rapidly damps with system impedance. Furthermore, current and voltages at the other MV feeders, the generators, and the loads terminals are sinusoidal and without voltage-quality issues.

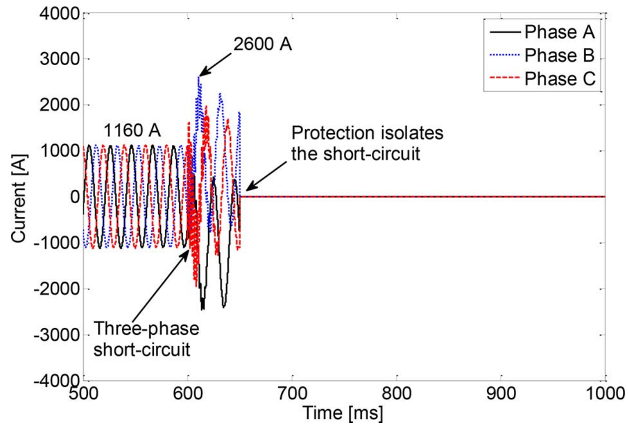

Fig. 8. Microgrid contribution to fault current during a fault at a generator terminal.

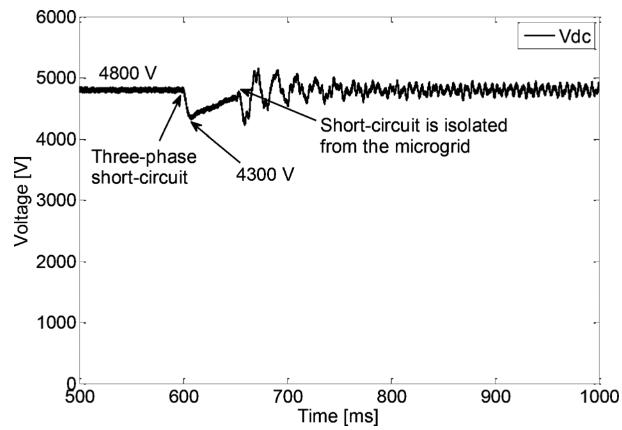

Fig. 9. Voltage at the dc bus when the microgrid contributes to fault current at a generator terminal.

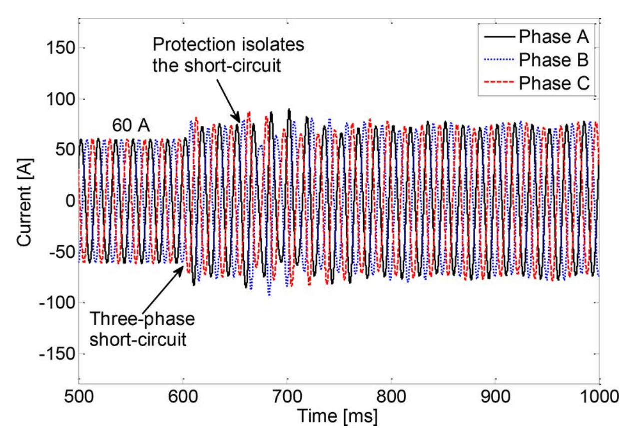

Fig. 10. Instantaneous current at the MV feeder interconnected with the faulted generator through the dc bus.

If the undervoltage fault detection was considered in this case, the short circuit would have been immediately isolated from the microgrid, eliminating oscillations at the dc bus.

C. Short Circuit to the Microgrid DC Bus

Due to the connection arrangement of the microgrid, a short circuit at any of the dc buses would result in the simultaneous loss of supply from a generator and a utility feeder. This

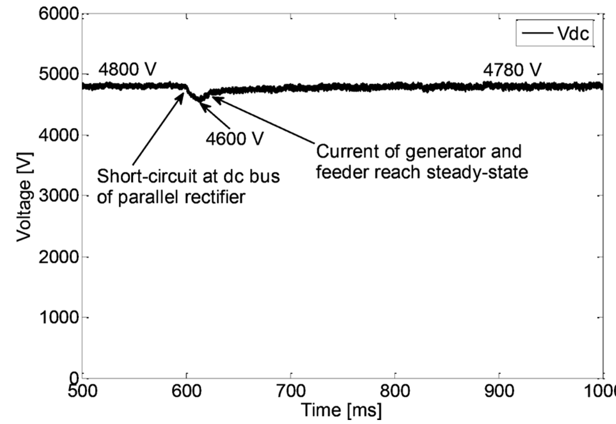

Fig. 11. Voltage at the dc bus of an unfaulted rectifier.

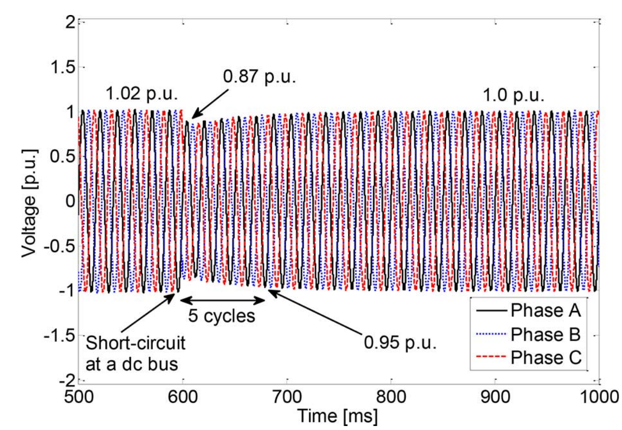

Fig. 12. Instantaneous voltage at the load terminal during a short circuit at a dc bus.

would appear to the microgrid systems as a double contingency—having one line and one generator out of service. In the event of such a fault, the remaining feeders and generators will be required to support the load previously supplied by the severed components. Moreover, it should be noted that the increase in power demand from the remaining feeders and generators might exceed the rating of the rectifiers, causing instability in the microgrid. Therefore, the rectifiers must be properly sized to account for this scenario. It is important for the microgrid installation not to cause power-quality problems or a substantial decrease in voltage levels during this type of scenario.

Simulation results show that when the short circuit appears at the dc bus, the power-electronics switches immediately disconnect, isolating the generator and the feeder. At this point, the dc voltage of the unfaulted rectifiers reduces as more current is drawn from its corresponding feeder and generator, see Fig. 11. Once the current reaches steady state, the rectifier dc voltages stabilize. The voltage waveforms of these feeders and generators remain unchanged throughout the simulation. The behavior of the voltage at the load terminals is shown in Fig. 12. As can be seen in the figure, the voltage drops from 1.02 to 0.87 p.u. for a brief period of time; approximately 5 cycles have a voltage deviation exceeding 5% from its nominal voltage which is considered an undervoltage [42].

V. Conclusion

The advantages of using nonsynchronous microgrids in heavily meshed secondary networks have been demonstrated. As shown in this paper, with transient simulations, a nonsynchronous microgrid isolated by means of a dc bus facilitates the integration of distributed generation because the grid and microgrid are electrically isolated. Therefore, the transient phenomena in one side do not propagate to the other. This is of paramount importance when the substation breakers operate close to their short-circuit rating.

The behavior of the grid and the microgrid has been investigated also in steady state with voltage reduction (CVR) comparing the losses and voltage profile in the presence and absence of the microgrid. The superiority of the dc microgrid compared with random distributed generation and no generation is made evident by the reduced number of buses with voltage violations.

References

[1] K. Strunz, E. Abbasi, and D. N. Huu, “DC microgrid for wind and solar power integration,” *IEEE J. Emerg. Sel. Topics Power Electron.*, vol. 2, no. 1, pp. 115–126, Mar. 2014.

[2] X. Yu, X. She, X. Zhou, and A. Q. Huang, “Power management for DC microgrid enabled by solid-state transformer,” *IEEE Trans. Smart Grid*, vol. 5, no. 2, pp. 954–965, Mar. 2014.

[3] R. Majumder, “A hybrid microgrid with DC connection at back to back converters,” *IEEE Trans. Smart Grid*, vol. 5, no. 1, pp. 251–259, Jan. 2014.

[4] R. Majumder, A. Ghosh, G. Ledwich, and F. Zare, “Power management and power flow control with back-to-back converters in a utility connected microgrid,” *IEEE Trans. Power Syst.*, vol. 25, no. 2, pp. 821–834, May 2010.

[5] F. Katiraei and M. R. Iravani, “Power management strategies for a microgrid with multiple distributed generation units,” *IEEE Trans. Power Syst.*, vol. 21, no. 4, pp. 1821–1831, Nov. 2006.

[6] H. Kakigano, Y. Miura, and T. Ise, “Low-voltage bipolar-type DC microgrid for super high quality distribution,” *IEEE Trans. Power Electron.*, vol. 25, no. 12, pp. 3066–3075, Dec. 2010.

[7] D. Chen, L. Xu, and L. Yao, “DC voltage variation based autonomous control of DC microgrids,” *IEEE Trans. Power Del.*, vol. 28, no. 2, pp. 637–648, Apr. 2013.

[8] D. Chen and L. Xu, “Autonomous DC voltage control of a DC microgrid with multiple slack terminals,” *IEEE Trans. Power Syst.*, vol. 27, no. 4, pp. 1897–1905, Nov. 2012.

[9] A. Kwasinski, “Quantitative evaluation of DC microgrids availability: Effects of system architecture and converter topology design choices,” *IEEE Trans. Power Electron.*, vol. 26, no. 3, pp. 835–851, Mar. 2011.

[10] T. Draglcevic, J. C. Vasquez, J. M. Guerrero, and D. Skrlec, “Advanced LVDC electrical power architectures and microgrids,” *IEEE Electrif.*, vol. 2, no. 1, pp. 54–65, Mar. 2014.

[11] S. Anand and B. G. Fernandes, “Reduced-order model and stability analysis of low-voltage DC microgrid,” *IEEE Trans. Ind. Electron.*, vol. 60, no. 11, pp. 5040–5049, Nov. 2013.

[12] S. Anand and B. G. Fernandes, “Optimal voltage level for DC microgrids,” in *Proc. 36th Annu. Conf. IEEE Ind. Electron. Soc.*, Nov. 2010, pp. 3034–3039.

[13] P. C. Loh, D. Li, Y. K. Chai, and F. Blaabjerg, “Autonomous operation of hybrid microgrid with AC and DC subgrids,” *IEEE Trans. Power Electron.*, vol. 28, no. 5, pp. 2214–2223, May 2013.

[14] P. C. Loh, D. Li, Y. K. Chai, and F. Blaabjerg, “Autonomous control of interlinking converter with energy storage in hybrid AC-DC microgrid,” *IEEE Trans. Ind. Appl.*, vol. 49, no. 3, pp. 1374–1382, May/Jun. 2013.

[15] J.-D. Park, J. Candelaria, L. Ma, and K. Dunn, “DC Ring-Bus Microgrid Fault Protection and Identification of Fault Location,” *IEEE Trans. Power Del.*, vol. 28, no. 4, pp. 2574–2584, Oct. 2013.

[16] J.-D. Park and J. Candelaria, “Fault detection and isolation in low-voltage DC-bus microgrid system,” *IEEE Trans. Power Del.*, vol. 28, no. 2, pp. 779–787, Apr. 2013.

[17] L. Roggia, L. Schuch, J. E. Baggio, C. Rech, and J. R. Pinheiro, “Integrated full-bridge-forward DC-DC converter for a residential microgrid application,” *IEEE Trans. Power Electron.*, vol. 28, no. 4, pp. 1728–1740, Apr. 2013.

[18] L. Xu and D. Chen, “Control and operation of a DC microgrid with variable generation and energy storage,” *IEEE Trans. Power Del.*, vol. 26, no. 4, pp. 2513–2522, Oct. 2011.

[19] X. Yu, X. She, and A. Huang, “Hierarchical power management for DC microgrid in islanding mode and solid state transformer enabled mode,” in *Proc. 39th Annu. Conf. IEEE Ind. Electron. Soc.*, Nov. 10–13, 2013, pp. 1656–1661.

[20] Y. Li, D. M. Vilathgamuwa, and P. C. Loh, “Design, analysis, and real-time testing of a controller for multibus microgrid system,” *IEEE Trans. Power Electron.*, vol. 19, no. 5, pp. 1195–1204, Sep. 2004.

[21] H. Kakigano, Y. Miura, T. Ise, T. Momose, and H. Hayakawa, “Fundamental characteristics of DC microgrid for residential houses with cogeneration system in each house,” in *Proc. IEEE Power Energy Soc. Gen. Meeting—Convers. Del. Elect. Energy 21st Century*, Jul. 2008, pp. 1–8.

[22] X. Feng, J. Liu, and F. C. Lee, “Impedance specifications for stable DC distributed power systems,” *IEEE Trans. Power Electron.*, vol. 17, no. 2, pp. 157–162, Mar. 2002.

[23] A. Sannino, G. Postiglione, and M. H. J. Bollen, “Feasibility of a DC network for commercial facilities,” *IEEE Trans. Ind. Appl.*, vol. 39, no. 5, pp. 1499–1507, Sep./Oct. 2003.

[24] D. Salomonsson and A. Sannino, “Low-voltage DC distribution system for commercial power systems with sensitive electronic loads,” *IEEE Trans. Power Del.*, vol. 22, no. 3, pp. 1620–1627, Jul. 2007.

[25] M. E. Baran and N. R. Mahajan, “DC distribution for industrial systems: Opportunities and challenges,” *IEEE Trans. Ind. Appl.*, vol. 39, no. 6, pp. 1596–1601, Nov./Dec. 2003.

[26] J. M. Guerrero, P. C. Loh, T.-L. Lee, and M. Chandorkar, “Advanced control architectures for intelligent microgrids—Part II: Power quality, energy storage, and AC/DC microgrids,” *IEEE Trans. Ind. Electron.*, vol. 60, no. 4, pp. 1263–1270, Apr. 2013.

[27] B. Zhao, Q. Yu, and W. Sun, “Extended-phase-shift control of isolated bidirectional DC-DC converter for power distribution in microgrid,” *IEEE Trans. Power Electron.*, vol. 27, no. 11, pp. 4667–4680, Nov. 2012.

[28] H. Kakigano, Y. Miura, and T. Ise, “Distribution voltage control for DC microgrids using fuzzy control and gain-scheduling technique,” *IEEE Trans. Power Electron.*, vol. 28, no. 5, pp. 2246–2258, May 2013.

[29] T. L. Vandoorn, B. Meersman, J. De Kooning, and L. Vandevelde, “Analogy between conventional grid control and islanded microgrid control based on a global DC-link voltage droop,” *IEEE Trans. Power Del.*, vol. 27, no. 3, pp. 1405–1414, Jul. 2012.

[30] H. Nikkhajoei and R. Iravani, “Steady-state model and power flow analysis of electronically-coupled distributed resource units,” in *Proc. IEEE Power Eng. Soc. Gen. Meeting*, Jun. 2007, pp. 24–28.

[31] Simulation Tool—OpenDSS. [Online]. Available: http://smartgrid.epri.com/SimulationTool.aspx

[32] DCG-EMTP (Development coordination group of EMTP) Version EMTP-RV, Electromagnetic Transients Program. [Online]. Available: http://www.emtp.com

[33] G. Y. Morris, S. Wong, and G. Joos, “Evaluation of the costs and benefits of microgrids with consideration of services beyond energy supply,” in *Proc. IEEE Power Energy Soc. Gen. Meeting*, Jul. 2012, pp. 1–9.

[34] P. N. Vovos, E. A. Kiprakis, A. R. Wallace, and G. P. Harrison, “Centralized and distributed voltage control: Impact on distributed generation penetration,” *IEEE Trans. Power Syst.*, vol. 22, no. 1, pp. 476–483, Feb. 2007.

[35] T. Senjyu, Y. Miyazato, A. Yona, N. Urasake, and T. Funabashi, “Optimal distribution voltage control and coordination with distributed generation,” *IEEE Trans. Power Del.*, vol. 23, no. 2, pp. 1236–1242, Apr. 2008.

[36] M. Diaz-Aguiló, J. Sandraz, R. Macwan, F. de León, D. Czarkowski, C. Comack, and D. Wang, “Field validated load model for the analysis of CVR in distribution secondary networks: Energy conservation,” *IEEE Trans. Power Del.*, vol. 28, no. 4, pp. 2428–2436, Oct. 2013.

[37] P. Chen, R. Salcedo, Q. Zhu, F. de León, D. Czarkowski, Z. P. Jiang, V. Spitsa, Z. Zabar, and R. Uosef, “Analysis of voltage profile problems due to the penetration of distributed generation in low-voltage secondary distribution networks,” *IEEE Trans. Power Del.*, vol. 27, no. 4, pp. 2020–2028, Oct. 2012.

[38] A. T. Davda, B. Azzopardi, B. R. Parekh, and M. D. Desai, “Dispersed generation enable loss reduction and voltage profile improvement in distribution network—Case study, Gujarat, India,” *IEEE Trans. Power Syst.*, vol. 29, no. 3, pp. 1242–1249, May 2014.
[39] R. Singh, F. Tuffner, J. Fuller, and K. Schneider, “Effects of distributed energy resources on conservation voltage reduction (CVR),” in *Proc. IEEE Power Energy Soc. Gen. Meeting*, Jul. 2011, pp. 1–7.
[40] *IEEE Standard Requirements for Secondary Network Protectors*, IEEE Standard C57.12.44, 2005.
[41] W. J. Lee, J. Cultrera, and T. Maffetone, “Application and testing of a microcomputer based network protector,” *IEEE Trans. Ind. Appl.*, vol. 36, no. 2, pp. 691–696, Mar./Apr. 2000.
[42] V. Spitsa, X. Ran, R. Salcedo, J. Martinez, R. Uosef, F. de León, D. Czarkowski, and Z. Zabar, “On the transient behavior of large-scale distribution networks during automatic feeder reconfiguration,” *IEEE Trans. Smart Grid*, vol. 3, no. 2, pp. 887–896, Jun. 2012.
[43] R. Sacedo, X. Ran, F. de León, D. Czarkowski, and V. Spitsa, “Long duration overvoltages due to current backfeeding in secondary networks,” *IEEE Trans. Power Del.*, vol. 28, no. 4, pp. 2500–2508, Oct. 2013.
[44] *IEEE Standard for Interconnecting Distributed Resources with Electric Power Systems*, IEEE Standard 1547, 2003 and Amendment 1 (IEEE Std. 1547a-2014).
[45] *IEEE Recommended Practices and Requirements for Harmonic Control in Electrical Power Systems*, IEEE Standard 519, 1992.
[46] A. McDonnell, “Electric power distribution methods and apparatus,” U.S. Patent US 8 183 714 B2, May 22, 2012.
[47] N. Miller and Z. Ye, “Report on distributed generation penetration study,” Golden, CO, USA, NREL/SR-560-34715, Aug. 2003, National Renewable Energy Laboratory.
[48] J. Sandraz, R. Macwan, M. Diaz-Aguiló, J. McClelland, F. de León, D. Czarkowski, and C. Comack, “Energy and economic impacts of the application of CVR in heavily meshed secondary distribution networks,” *IEEE Trans. Power Del.*, vol. 29, no. 4, pp. 1692–1700, Aug. 2014.
[49] M. Shahidehpour and M. Khodayar, “Cutting the campus energy costs with hierarchical control,” *IEEE Electrif. Mag.*, vol. 1, no. 1, pp. 40–56, Sep. 2013.
[50] DOE Microgrid Workshop Report., Sep. 2012. [Online]. Available: http://energy.gov/oe/downloads/2012-doe-microgrid-workshop-summary-reportseptember-2012, Office of Electricity Delivery and Energy Reliability Smart Grid R&D Program
[51] CIGRÉ Working Group C 6.22, “Microgrids evolution roadmap,” Paris, France, 2010.
[52] S. Flank, “GridLink: A new power electronics interconnection technology study,” Final Report, Prepared for the New York State Energy Research and Development Authority (NYSERDA), Nov. 2014.

Reynaldo Salcedo (S’13), photograph and biography not available at the time of publication.

Abdullah Bokhari, photograph and biography not available at the time of publication.

Marc Diaz-Aguiló, photograph and biography not available at the time of publication.

Nanzhu Lin, photograph and biography not available at the time of publication.

Tianqi Hong, photograph and biography not available at the time of publication.

Francisco de León (F’15), photograph and biography not available at the time of publication.

Dariusz Czarkowski (M’97), photograph and biography not available at the time of publication.

Shalom Flank, photograph and biography not available at the time of publication.

Alan McDonnell, photograph and biography not available at the time of publication.

Resk Ebrahem Uosef (M’10), photograph and biography not available at the time of publication.